PROCEEDINGS OF SPIE

SPIEDigitalLibrary.org/conference-proceedings-of-spie

High-power/energy large mode area tapered fiber amplifiers

Roy, V., Grenier, P., Desbiens, L., Deshaies, S., Deladurantaye, M., et al.

V. Roy, P. Grenier, L. Desbiens, S. Deshaies, M. Deladurantaye, P. Paradis, M. Boivin, B. Labranche, A. Proulx, Y. Taillon, "High-power/energy large mode area tapered fiber amplifiers," Proc. SPIE 11665, Fiber Lasers XVIII: Technology and Systems, 1166509 (5 March 2021); doi: 10.1117/12.2584194

SPIE.

Event: SPIE LASE, 2021, Online Only

High-power/energy large mode area tapered fiber amplifiers

V. Roy*, P. Grenier, L. Desbiens, S. Deshaies, M. Deladurantaye,
P. Paradis, M. Boivin, B. Labranche, A. Proulx and Y. Taillon

INO, 2740 Einstein, Québec, QC, G1P 4S4 Canada

ABSTRACT

A short-pulse Yb-doped fiber laser based on a master oscillator and power amplifier scheme is reported to yield an average power exceeding 500 W and pulse energy over 1 mJ. The final amplifier stage features a polarization-maintaining, large mode area tapered fiber with core/cladding diameters of 35/250 µm and 56/400 µm at each end of the flared section. The latter yields excellent optical conversion efficiency, near diffraction-limited output, narrow spectral linewidth and high polarization extinction ratio. The threshold for the onset of stimulated Raman scattering was further investigated using a pulsed seeder with ps-ns digitally programmable waveforms. Besides, no indication for transverse mode instability could be observed below the stimulated Raman scattering threshold, as beam quality M^2 was measured < 1.3 and no fluctuations were further detected from photodiode time-traces of near-field laser beam samples.

Keywords: Fiber Amplifier, Large Mode Area, Ytterbium, Taper, Transverse Mode Instability, Photodarkening.

1. INTRODUCTION

Transverse mode instability (TMI) has received much attention in recent years because of the limitation it sets on the output power of fiber amplifiers. As the heat load becomes significant, the refractive index profile of the waveguide also changes, consistent with the underlying longitudinal/transverse inversion along the active fiber. In some circumstances, the latter leads to mode coupling beyond a certain threshold, with periodic and eventually random energy transfer from the fundamental mode to undesirable higher-order modes (HOMs). Deterioration of beam quality and beam pointing occurs as a result of mode coupling then taking place, with fluctuations timescales determined by transient thermal diffusion process. Various mitigation strategies have been discussed, relying on either passive or active methods, some intrinsic to the active fiber and others related with the system operating conditions. A comprehensive review of the literature and the various mitigation methods has been published recently [1].

Specialty optical fibers have experienced significant progress in the last decade or so, while several concepts of large mode area fibers have been proposed to overcome the limitations set by nonlinear effects that stems from amplification of ultrashort optical pulses. As effective as they may be with preventing the onset of nonlinear effects such as stimulated Raman scattering (SRS), most will fail to keep up with the uptrend in power scaling as seen in the laser industry. In the literature, the threshold for the onset of TMI has been reported to scale roughly with the inverse square of the fiber core diameter. While most kW lasers rely on small-core 20/400 LMA fibers, ultrafast lasers instead feature active fibers with much larger cores (≥ 30 µm), in which case keeping diffraction limited output is often a challenge. For instance, TMI thresholds as low as a few 100s W were reported for fiber rods with very large mode areas. Nevertheless, scaling laser average power of ultrafast systems with coherent beam combining of several amplifier channels has led to remarkable results in recent years, and in some cases with a single fiber strand featuring multiple cores.

Another interesting trend consists in using a tapered active fiber with only the fundamental mode being amplified along the flared section connecting both ends of the fiber. LMA fibers drawn as tapers during fiber fabrication have attracted much attention in recent years [2-5], fulfilling all expectations thus far with high average power and diffraction-limited output. Here we report the fabrication of a new Yb-doped tapered fiber, with cladding absorption inferior to previous generations, and TMI threshold now exceeding 500 W. The polarization maintaining fiber will prove useful for high power ultrafast amplifiers as well as laser harmonics generation. In the following, a brief outline of the LMA tapered fiber properties and its performances as a laser amplifier are described in section 2. A detailed account of the onset of TMI instability is further given in section 3, with the latter to be followed by concluding remarks.

* vincent.roy@ino.ca / www.ino.ca

Fiber Lasers XVIII: Technology and Systems, edited by Michalis N. Zervas, Proc. of SPIE
Vol. 11665, 1166509 · © 2021 SPIE · CCC code: 0277-786X/21/$21
doi: 10.1117/12.2584194

2. TAPERED FIBER AMPLIFIERS

2.1 LMA Tapered Fiber

LMA fibers with different levels of pump absorption were fabricated, starting off from glass preforms fabricated from conventional MCVD and next with different ytterbium concentrations at solution doping. The two fibers have molar concentrations of phosphorous and aluminum oxides adjusted in proportion with ytterbium content, i.e. to achieve high concentration Yb doping and keep photodarkening losses at a minimum. Both fibers were pulled as tapers at the drawing tower, with near identical core/cladding diameters in each section. Optical properties as well as physical characteristics for the two fibers are listed in Table 1. The main difference between both fibers lies in the cladding absorption, i.e. with absorption at 915 nm measured at 2.2 dB/m for fiber #1 and 2.7 dB/m for fiber #2. The length of the flared section is 0.7 m while the total fiber length (including straight sections on each side) falls between 1.8-2.4 m, depending on the cladding absorption and the amount of unabsorbed pump power that can be managed safely after the laser amplifier. Birefringence provided by the Panda-type stress rods was measured at $1.8 \cdot 10^{-4}$ ensuring superior polarization extinction.

The fundamental mode effective area A_{eff} at the output of the flared section falls in the range of 850-950 μm^2 from calculations based on the actual refractive index profiles. In the case of fiber #1 it is found near the lower end of this range while for fiber #2 it lies near the superior end. Besides the refractive index of fiber #1 features a graded-like parabolic profile whereas fiber #2 assumes a more step-like profile. In the fabrication process ytterbium ions were confined to the core center, with confinement ratios (≈ 0.7) nearly the same for both fibers. Dopant confinement is known as a mitigation method for TMI, effectively reducing the strength of the mode coupling induced by the heat load along the fiber. Additionally, the inner cladding layer with trench-like depressed index enhances the bending-induced losses for higher-order modes, as detailed in a previous report [5].

Fiber endcaps were spliced at the end of fiber #1 and fiber #2 to reduce the peak laser fluence on the AR-coated surface and avoid catastrophic damage. The endcap aperture (Ø10 mm) was made large enough to have the pump light launched from this end for counter-pumping. Each fiber samples were fitted on a cold plate mount with recirculating liquid coolant for efficient dissipation of waste heat given the significant heat load developing along the fiber. The fiber coiling was restricted to large diameters (~ 30-40 cm) to avoid excessive reduction of the mode area. The fiber samples were also potted with a thermally conductive adhesive to increase cooling. The fiber amplifier assemblies were tested according to a wide range of environmental conditions, both operational and survival. Besides, the amplifier modules have shown very minimal decline in output power during life tests spanning over 3000 hours, except for spontaneous drops due to failures of individual emitters in pump laser diodes.

Table 1 – Characteristics of the large mode area tapered fibers.

OPTICAL PROPERTIES		DATA
Core Numerical Aperture		0.065
Cladding Numerical Aperture		0.50
Cladding Absorption / 915 nm	[dB/m]	2.2-2.7
Cladding Absorption / 976 nm	[dB/m]	8.8-10.8
Birefringence		$1.8 \cdot 10^{-4}$
PHYSICAL CHARACTERISTICS		**DATA**
Small Core Diameter	[μm]	35
Small Cladding Diameter	[μm]	250
Large Core Diameter	[μm]	56
Large Cladding Diameter	[μm]	400
Coating Diameter	[μm]	520

2.2 MOPA Laser System

The amplifier modules based on tapered fibers #1 and #2 were tested in a master oscillator and power amplifier configuration with different emission regimes (see Fig. 1). Pulse generation in the master oscillator is first initiated from direct current modulation of a wavelength-stabilized laser diode emitting at 1064 nm. Digitally programmable nanosecond optical pulses were produced with constant pulse duration regardless of pulse repetition frequency, which was set here to 2.5 ns for frequencies between 200-500 kHz. Synchronous phase modulation is then superimposed onto the nanosecond pulses using an electro-optic modulator to lessen stimulated Brillouin scattering (SBS) in the fiber amplifiers downstream. Phase modulation is set such as to effectively suppress SBS and yet avoid excessive broadening of the laser linewidth (≈ 0.5 nm). Alternatively, picosecond pulses could be generated by inserting a narrowband fiber Bragg grating (FBG) with very steep edges thereafter (not shown in Fig. 1). The peak reflectivity of the FBG is offset from the signal carrier frequency so the phase-modulated light wave gets reflected only once every cycle, for a very short time, on the rising edge of the modulation signal. The resulting pulse duration could be adjusted close to a minimum (≈ 35 ps) simply by increasing/decreasing the phase modulation amplitude while tuning the temperature of either the seed laser diode or FBG.

Subsequent to ns/ps pulse generation and prior to the last stage along the amplifier chain lies two pre-amplifier stages, the first one based on a 5-µm Yb-doped PM fiber (INO Yb401-PM) and the second one on a 10-µm Yb-doped multi-clad PM fiber (INO Yb-MCOF-10/125-0.8-1.6-PM). The single-mode output is spliced to the final amplifier stage (INO Yb-MCOF-35/250-56/400-07-2.2-T0.7-PM) using a mode field adapter and seeded with an average power in the range 0.2-2 W (depending on the laser regime). As mentioned before the fiber is packaged on a liquid-cooled cold plate and fitted with an endcap to sustain high optical powers (see Section 2.1). Optical pumping was arranged for using 7 x 100W laser diodes with 976-nm VBG wavelength stabilization, all of them combined in a single output using a multimode fiber combiner with 220/242µm and 0.22/0.46NA. Aspheric optics were used to launch the pump light at the same time as collecting signal light coming through the end of the fiber amplifier module given the counter-pumping scheme.

Absolute average power as high as 610W and corresponding optical efficiency of 85% was obtained at the amplifier output with fiber #1 considering the limited power available for optical pumping of the final stage (and further without roll-off, see Section 3). Besides, average powers achieved either with fiber #1 or fiber #2, before TMI or SRS threshold were exceeded, are summarized in Table 2 for both quasi-CW and pulsed laser emission. Peak power and pulse energy presumed for the latter regimes are listed along as well. For instance, average power was measured in the range of 255-490 W for nanosecond pulses with repetition frequency set between 200-500 kHz (see Fig. 2), i.e. before power in the SRS Stokes-shifted frequency exceeded 0.1% (a rather strict criterion).

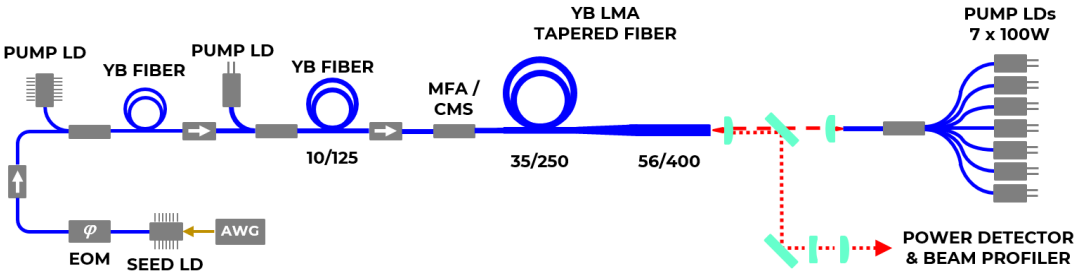

Figure 1 – Schematic representation of the laser system (AWG: arbitrary waveform generator; LD: laser diode; EOM: electro-optic modulator; MFA: mode-field adapter; CMS: cladding mode stripper).

Table 2 – Laser parameters at the amplifier output according to various operating regimes.

Laser Emission	Average Power	Pulse Duration	Repetition Frequency	Peak Power	Pulse Energy	Threshold Limit
QCW / fiber #1	510 W	-	-	-	-	TMI
ns / fiber #1	255-490 W	2.2 ns	200-500 kHz	420-540 kW	1.0-1.3 mJ	SRS
ps / fiber #2	300-330 W	35 ps	7.5-10.0 MHz	0.84-1.02 MW	33-40 µJ	SRS

The pulse waveforms also show evidence of saturation as pulse duration now seems shorter (2.2 ns instead of 2.5 ns initially) while pulse leading (trailing) edge become more (less) steep (see inset in Fig. 2). Saturation energy for fiber amplifiers can be calculated according to $E_{sat} = Ahv/\Gamma(\sigma_{abs}+\sigma_{emi})$, where A is the dopant area, Γ is the mode overlap with the dopant area and $\sigma_{abs/emi}$ are the Yb absorption/emission cross sections. E_{sat} is estimated at 0.4 mJ and 1.0 mJ for the small and large sections of the tapered fiber, respectively. The latter estimates agree fairly well with calculations performed from pulse waveforms measured before/after the last amplifier stage, with $E_{sat} \approx 0.7$ mJ for the entire fiber span. The latter also places the extracted energies with ns pulses at about twice the "mean" saturation energy of the tapered fiber amplifier. Peak powers inferred from the pulse waveforms and pulse energy were found in the range 420-540 kW, using a constant factor $cnst \approx 0.92$ in the relation $P_{peak} = cnst \cdot E/\tau_{FHWM}$.

On the other hand, the amplification of ps pulses yielded peak powers much higher, i.e. 0.84-1.02 MW, again with the same threshold considered for SRS onset (≈ 0.1%, see Fig. 3). One reason for such a large difference with results from ns pulse amplification is the shorter length used for fiber #2 (~30% less). Another reason as well is the seed power which

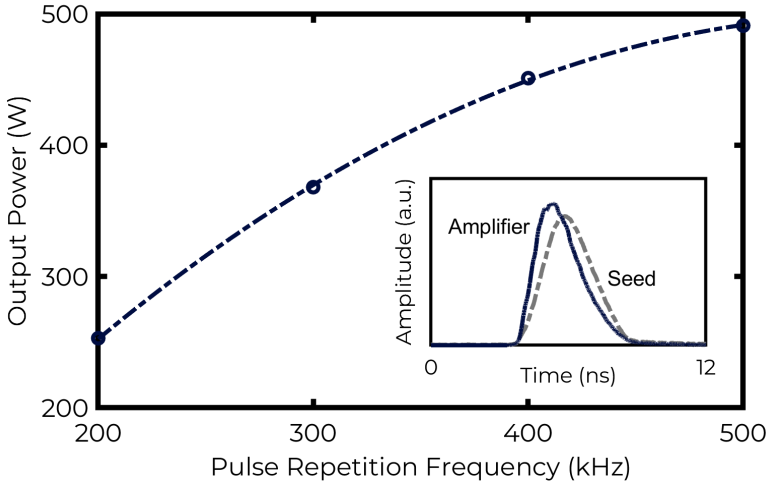

Figure 2 – Amplifier output power vs. oscillator pulse repetition frequency with ≲ 0.1% power in the SRS Stokes frequency band. Inset: pulse waveforms before/after the tapered fiber amplifier with output power of 440 W and pulse repetition frequency of 400 kHz.

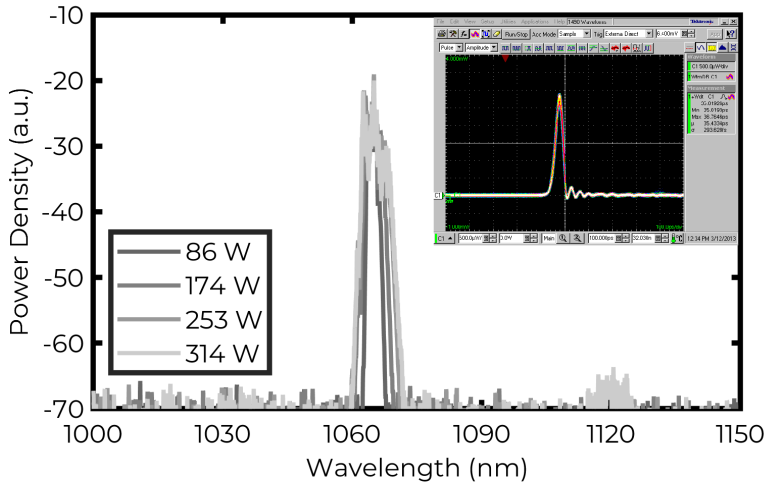

Figure 3 – Amplifier output pulse spectra with increasing laser average powers. Inset: optical pulse waveforms with 35-ps duration (pulse repetition frequency is 10 MHz).

was 2-3x smaller with ps pulses compared with the ns pulses. With average powers exceeding 300 W the gain provided by the last amplifier stage was calculated to be superior to 30 dB. The constant factor *cnst* ≈ 0.89 was assumed in calculating the pulse peak power from relation $P_{peak} = cnst \cdot E/\tau_{FHWM}$ given the temporal shape of the pulses (see inset in Fig. 3). Besides broadening induced by self-phase modulation is still manageable for most laser applications, with spectral linewidth at -20 dB close to 7 nm.

The polarization of light was measured at several times during the entire series of tests considering all three laser regimes. The polarization extinction ratio was calculated to exceed 16 dB in all conditions at the amplifier output except beyond the TMI threshold. The beam quality factor (M^2) was also characterized in each instance and near diffraction-limited output was obtained with $M^2 < 1.3$, except beyond the TMI threshold. In addition, intensity fluctuations were monitored from time traces using a photodiode introduced in front of a sample of the imaged beam as described in [6]. The output fluctuations seen near TMI threshold and beyond because of the mode beatings is known to come along with a sudden increase in the normalized standard deviation and feature distinct spectral signature.

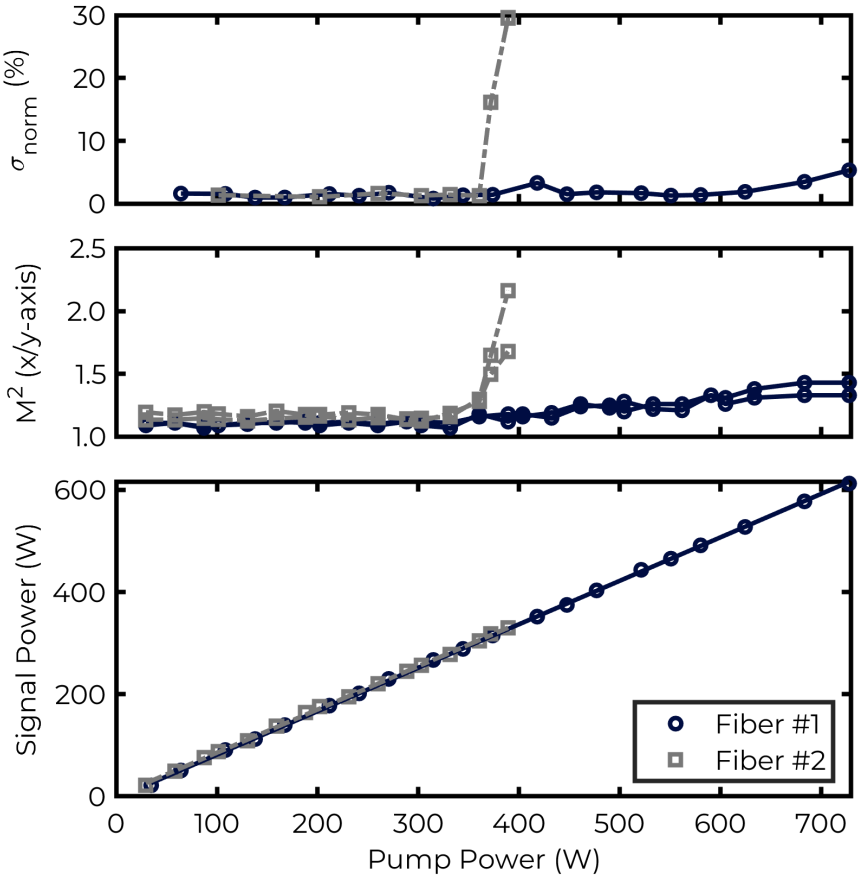

Figure 4 – Laser amplifier output power (bottom), beam quality (middle) and normalized standard deviation of intensity fluctuations from photodiode time-traces of near-field laser beam samples (top), with LMA tapered fiber #1 and fiber #2.

3. TRANSVERSE MODE INSTABILITY

The route to transverse mode instability is generally described as a two-step process, with successive transitions from stable laser emission to periodic fluctuations and next to random (or seemingly chaotic) fluctuations as laser power is increased further beyond the instability threshold [6-7]. The transition region usually features a set of discrete and equally spaced frequency peaks from Fourier analysis of photodiode time traces. The random region, instead, is characterized by a noise-like spectrum which spreads over a broad frequency range. As it stands, the threshold is established as the limit beyond which fluctuations show up on top of stable laser emission and grow exponentially, so we can safely ignore the random region beyond this threshold. Accordingly, both fibers were tested to power levels such that the threshold could be clearly identified. Still the pump power available (≈ 700 W) was simply not enough to move way beyond this point for fiber #1.

As seen from Figure 4, fiber #1 and fiber #2 feature very distinct thresholds, with the former almost twice as high as the latter. Besides, while a very steep transition is seen for fiber #2, the picture is quite different with fiber #1 as the transition occurs much more progressively. Not only does TMI threshold differ drastically between both fibers, but also

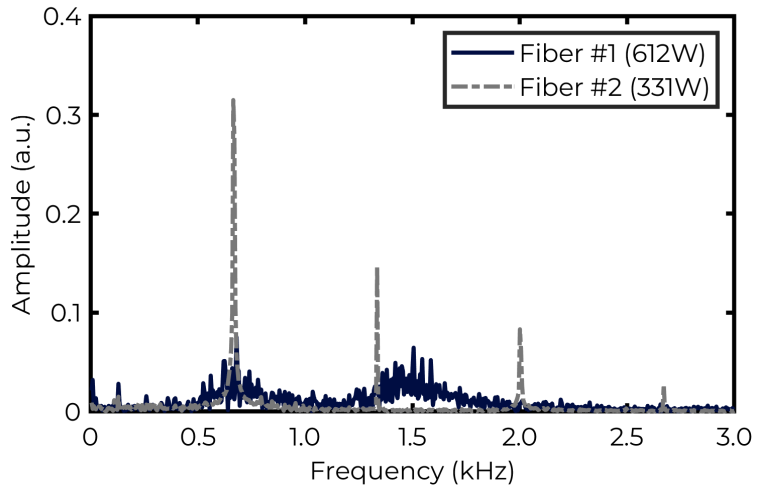

Figure 5 – Fourier spectra from time traces of near-field laser beam samples for maximum average powers from both laser amplifier fibers.

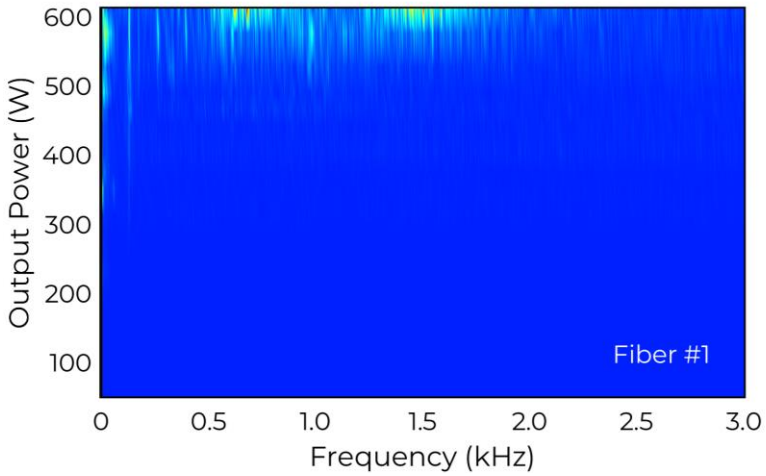

Figure 6 – Fourier spectra from time traces of near-field laser beam samples for increasing average power from amplifier output (fiber #1).

the Fourier spectra of photodiode time traces beyond this point show very different signature. Fluctuations past the TMI threshold for fiber #2 is characterized by sharp frequency peaks, i.e. near 667 Hz and its harmonics (see Fig. 5), with an upper frequency limit at approximately 3.3 kHz. The latter is consistent with the analysis in [6], where the thermal diffusion time and subsequent frequency limit is established from the general temperature distribution of a solid rod as $\nu_{lim} = 4\kappa/(C \cdot \rho \cdot MFD^2)$, where κ (= 1.38 W/m·K) is the thermal conductivity of fused silica, C (= 703 J/kg·K) is the heat capacity, ρ (= 2201 kg/m^3) is the density and MFD = 34 µm is the mode-field diameter, with $\nu_{lim} \approx 3$ kHz.

Meanwhile fluctuations beyond the TMI threshold for fiber #1 exhibit noise-like frequency distribution more or less at the same frequencies (see Fig. 5-6), although with much reduced amplitude. Such a spectral distribution is very different from the one measured with fiber #2, and for that matter from usual TMI reports in the literature. The noise-like spectra most probably result from random-like wandering of the beam centroid, as the observations performed with a CCD camera suggest. Also noteworthy is the fact that HOMs never quite show up for fiber #1, as clear and obvious as with fiber #2, but this is perhaps due to insufficient pump power. Nevertheless, the threshold value for the onset of TMI is evaluated at ≈ 512 W, as defined by the first derivative of the normalized standard deviation with output power $d\sigma_{norm}/dP_{output} \equiv 0.1$‰/W [6] (with the one outlier data point left aside from exponential curve fitting, see Fig. 7). In addition, some low frequency components were noticed, i.e. ≈ 130 Hz and successive harmonics, the origin of which is not yet fully understood.

The TMI threshold for fiber #1 compares favorably to other specialty fibers, even more so considering the greater heat load developing along the fiber, with the quantum defect between the pump (976 nm) and signal (1064 nm) close to 60% larger than most reports where signal is tuned near 1030 nm. Also, TMI threshold was neither observed to lessen with successive tests performed using the same fiber sample nor during extended tests. For instance, a life test stretching over 100 hours did not show significant power decay. Such outstanding performance is in part due to exceptional resistance of the fiber against photodarkening with suitable molar ratio of phosphorous and aluminum oxides [8-9].

Accordingly, losses from photodarkening is believed to contribute little in the so-called “heat-load bucket” [10], an informal concept introduced to portray the heat generated in a fiber amplifier before the onset of TMI. Following the latter, almost all heat generated in the amplifier may be considered productive, e.g. induced by the quantum defect associated with the radiative transition. Besides numerically solving the laser rate equations yields average and peak heat loads along the amplifier fiber near 20 W/m and 100 W/m, respectively, with the latter taking place at the distal end given the counter-pumping scheme. The estimated average heat load is less than the value often quoted in the literature near threshold, according to the same heat-load bucket concept. This is not surprising since counter-pumping is known to increase the threshold, in part due to the gain saturation somewhat levelled along the fiber, which in turn makes the system less prone to TMI build-up from noise.

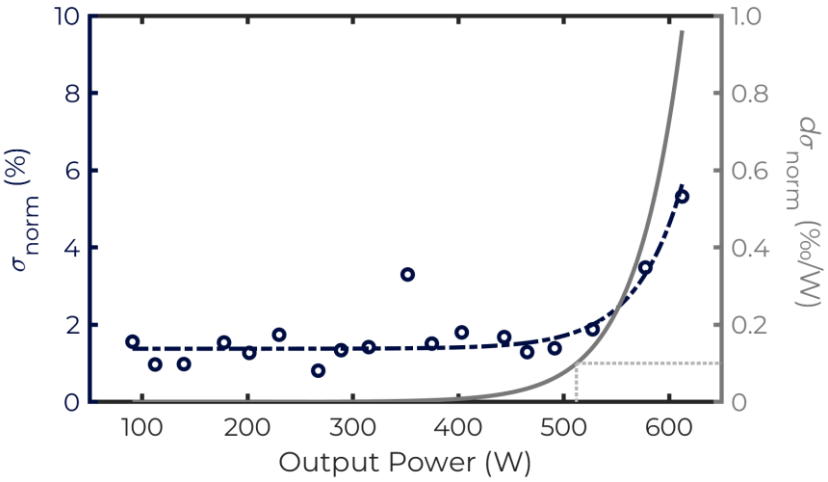

Figure 7 – Normalized standard deviation of photodiode time traces and exponential fit (left) along with the first derivative with respect to amplifier output power (right).

4. CONCLUSION

In recent years tapered fibers have stood out as a truly scalable concept for high energy amplifiers, with reports of MW-mJ diffraction-limited outputs and now with very high average powers. The flared waveguide geometry has proven beneficial in mitigating both transverse mode instabilities and nonlinear effects. The increased gain saturation at the small end lessens mode coupling from underlying heat load all the while the expanded mode area at the large end increases the threshold for nonlinear effects such as stimulated Raman scattering. Accordingly, large mode area tapered fibers seem perfectly matched for amplification of pulsed lasers with both high average and peak powers. Besides the confinement of ytterbium dopants and low-photodarkening silica glass further help reduce the strength of the long-period index grating, thus effectively holding back the onset of transverse mode instability. Here for instance an average laser power exceeding 500 W could be achieved free of instabilities, i.e. with near diffraction-limited laser output. Laser systems with LMA tapered fibers as described herein would no doubt prove advantageous for laser materials processing applications, for instance with high-power ultrafast lasers or else for high-power VIS/UV harmonics generation.

REFERENCES

[1] Jauregui, C., Stihler, C., Limpert, J., "Transverse Mode Instability," Adv. Opt. Photon. 12, 429-484 (2020).

[2] Filippov, V., Chamorovskii, Y., Golant, K., Vorotynskii, A., Okhotnikov, O., "Optical amplifiers and lasers based on tapered fiber geometry for power and energy scaling with low signal distortion," in Fiber Lasers XIII: Technology, Systems and Applications, ed. J. Ballato, Proc. of SPIE 9728, 97280V (2016).

[3] Bobkov, K., Andrianov, A., Koptev, M., Muravyev, S., Levchenko., A., et al., "Sub-MW peak power diffraction-limited chirped-pulse monolithic Yb-doped tapered fiber amplifier," Opt. Express 25, 26958-26972 (2017).

[4] Roy, V., Paré, C., Labranche, B., Laperle, P., Desbiens, L., et al., "Yb-doped large mode area tapered fiber with depressed cladding and dopant confinement," in Fiber Lasers XIV: Technology, Systems and Applications, eds C. A. Robin and I. Hartl, Proc. of SPIE 10083, 1008314 (2017).

[5] Shi, C., Zhang, H., Wang, X., Zhou, P., Xu, X., "kW-class high power fiber laser enabled by active long tapered fiber," High Power Laser Sci. Eng. 6, e16 (2018).

[6] Otto, H.-J., Stutzki, F., Jansen, F., Eidam, T., Jauregui, C., et al., "Temporal dynamics of mode instabilities in high-power fiber lasers and amplifiers," Opt. Express 20, 15710-15722 (2012).

[7] Johansen, M. M., Laurila, M., Maack, M.D., Noordegraaf, D., Jakobsen, C., et al., "Frequency resolved transverse mode instability in rod fiber amplifiers," Opt. Express 21, 21847-21856 (2013).

[8] Jauregui, C., Stutzki, F., Tünnermann, A., Limpert, J., "Thermal analysis of Yb-doped high-power fiber amplifiers with Al:P co-doped cores," Opt. Express 26, 7614-7624 (2018).

[9] Haarlammert, N., Kuhn, S., Hupel, C., Nold, J., Schulze, S., et al., "Analysis of fabrication techniques and material systems for kW fibers limited by TMI," in Fiber Lasers XVII: Technology and Systems, ed. L. Dong, Proc. of SPIE 11260, 1126026 (2020).

[10] Jauregui, C., Otto, H.-J., Stutzki, F., Limpert, J., Tünnermann A., "Simplified modelling the mode instability threshold of high power fiber amplifiers in the presence of photodarkening," Opt. Express 23, 20203-20218 (2015).